Molecular Crystals and Liquid Crystals Science and Technology. Section A. Molecular Crystals and Liquid Crystals
Publication details, including instructions for authors and subscription information:
http://www.tandfonline.com/loi/gmcl19

Thin Films of BEDT-TTF and BEDO-TTF Radical Cation Salts

J. Moldenhauer [a], U. Niebling [a], T. Ludwig [a], B. Thoma [a], D. Schweitzer [a], W. Strunz [b], H. J. Keller [b], P. Bele [c] & H. Brunner [c]

[a] 3. Physikalisches Institut der Universitat Stuttgart, Pfaffenwaldring 57, 70569, Stuttgart, Germany

[b] Anorganisch-Chemisches Institut der Universitat Heidelberg, Im Neuenheimer Feld 270, 69120, Heidelberg, Germany

[c] Max-Planck-Institut fur medizinische Forschung, AG Molekülkristalle, Jahnstr. 29, 69120, Heidelberg, Germany

Version of record first published: 24 Sep 2006.

To cite this article: J. Moldenhauer , U. Niebling , T. Ludwig , B. Thoma , D. Schweitzer , W. Strunz , H. J. Keller , P. Bele & H. Brunner (1996): Thin Films of BEDT-TTF and BEDO-TTF Radical Cation Salts, Molecular Crystals and Liquid Crystals Science and Technology. Section A. Molecular Crystals and Liquid Crystals, 284:1, 161-182

To link to this article: http://dx.doi.org/10.1080/10587259608037920

Mol. Cryst. Liq. Cryst., 1996, Vol. 284, pp. 161–182
Reprints available directly from the publisher
Photocopying permitted by license only

THIN FILMS OF BEDT-TTF AND BEDO-TTF RADICAL CATION SALTS

J. MOLDENHAUER, U. NIEBLING, T. LUDWIG, B. THOMA, and D. SCHWEITZER
3. Physikalisches Institut der Universität Stuttgart,
Pfaffenwaldring 57, 70569 Stuttgart, Germany

W. STRUNZ and H. J. KELLER
Anorganisch-Chemisches Institut der Universität Heidelberg,
Im Neuenheimer Feld 270, 69120 Heidelberg, Germany

P. BELE and H. BRUNNER
Max-Planck-Institut für medizinische Forschung, AG Molekülkristalle,
Jahnstr. 29, 69120 Heidelberg, Germany

Abstract

In this communication we describe the fabrication and characterization of thin films of the radical cation salts α-, α_t-(BEDT-TTF)$_2$I$_3$ and (BEDO-TTF)$_{2.4}$I$_3$. Thin films of these compounds were made by evaporation of the salts in high vacuum onto several substrates. They were characterized by X-ray diffraction, scanning electron microscopy, infrared absorption, Raman scattering, dc-conductivity measurements and magnetically modulated microwave absorption. Depending on the temperature of the substrate and the evaporation rate, the films of α-(BEDT-TTF)$_2$I$_3$ exhibit different degrees of microcrystallinity which under the right conditions can be strongly reduced to obtain relatively smooth, completely covering films. Additionally such films have a high degree of orientation with respect to the substrate plane. The conversion into films of the superconducting α_t-phase is possible and the high orientation is maintained. Due to grain boundaries, the dc-conductivity is thermally activated, but the single grains are superconducting. The best results in the fabrication of smooth, completely covering films were obtained with (BEDO-TTF)$_{2.4}$I$_3$ on NaCl single crystals. Here the orientation of the donor molecule with respect to the substrate plane is different from the one found in the (BEDT-TTF)$_2$I$_3$ salts .

INTRODUCTION

Radical cation salts of the organic donor BEDT-TTF (Bis(ethylene-dithiolo)-tetrathiafulvalene) and BEDO-TTF (Bis(ethylene-dioxy)tetrathiafulvalene) have been widely investigated since their first synthesis[1,2]. A lot of quasi-two-dimensional organic conductors and superconductors have been synthesized since then[3]. Depending on the

anions different unit cells and types of donor arrangements of the molecules in them were be found which leads to different transport properties from semiconducting over metallic to superconducting.

In the present paper we restrict ourselves to the iodine salts of BEDT-TTF and BEDO-TTF. For the $(BEDT\text{-}TTF)_2I_3$ salts many crystallographic phases have been found, two of which are important here. The first is α-$(BEDT\text{-}TTF)_2I_3$, which is a metal at room temperature - the room temperature conductivity lies between 60 and 250 S/cm - and has a sharp metal-insulator transition at 135 K [4,5]. This α-phase can be converted into α_t-$(BEDT\text{-}TTF)_2I_3$ [6,7] (by tempering the crystals for 2 or 3 days at 75 °C), which is a metal down to 8 K, where it becomes superconducting. The first organic metal of BEDO-TTF reported was its iodine salt $(BEDO\text{-}TTF)_{2.4}I_3$ [2], which is a metal down to lowest temperatures.

Because of the great variety of these organic metals they might be interesting for future molecular electronics. The preparation of thin films and the investigation of their properties might reveal, how these radical cation salts can be used as building blocks for molecular electronics e.g. as conducting interfaces between molecular units with different functions. First results in preparing thin films of $(BEDT\text{-}TTF)_2I_3$ have already been presented by Kawabata et al.[8,9].

EXPERIMENTAL

Film Preparation

Ground crystals of the respective radical cation salt (5-10 mg) were evaporated from a Knudsen cell. The base pressure in the vacuum chamber was 10^{-8} mbar. The source temperature during evaporation was kept between 130 °C and 200 °C, depending on the radical cation salt and the desired deposition rate. The deposition rate was varied between 0.2 and 1.5 A, while the substrate temperatures ranged from 300 K to 150 K. The distances between the source and the substrates were between 8 cm and 30 cm.

Mass spectra of $(BEDT\text{-}TTF)_2I_3$ powder at different temperatures between 50 °C and 270 °C have shown that the evaporation of iodine starts at 70 °C and a significant evaporation of BEDT-TTF does not begin below 170 °C. If larger amounts of the radical cation salt have been reduced to neutral BEDT-TTF - which evaporates above 205 °C - an excess quantity of neutral BEDT-TTF in the film can be avoided by keeping the source temperature below 200 °C. Mass spectra show as well that above 220 °C the BEDT-TTF molecule is destroyed.

The substrates - mostly quartz glass and silicon wafers - have been cleaned in different stages in acetone and ethanol in an ultrasonic bath, afterwards rinsed with demineralized water and dried with N_2. Other substrates like mica and NaCl single crystals have

been cleaved in order to obtain clean surfaces. After insertion into the vacuum, all substrates have been heated at 150 °C for 10 to 20 hours.

Characterization

The characterization of the films was performed with various techniques. X-ray diffraction (XRD) spectra were taken with a commercial Siemens D 500 diffractometer, scanning electron microscopy (SEM) was performed with a Zeiss DSM 940 A.

The dc-conductivity of the films was measured with the standard four-probe method with gold contacts (contact distance 0.2 mm) evaporated onto the film. To avoid errors when the film resistance was high, data were recorded only at temperatures at which the resistance of the films was at least ten times smaller than the impedance of the nanovoltmeter (Keithley 181).

Infrared absorption spectroscopy was carried out with a Bomem DA 3.02 Fourier transform spectrometer. Spectra were calculated from 2000 coadded scans with a resulting resolution of 1 cm^{-1}. To increase signal-to-noise-ratio, a reflection setup for near-normal incidence with a mirror behind the substrate was used, allowing the beam to pass the film twice.

Raman spectra were measured either with a krypton ion laser working at 676.4 nm or an argon laser working at 488.0 nm, the probe mounted on the sample block of a continuous flow cryostat at 50 K, with a double monochromator and a photoncounting system.

The magnetically modulated microwave absorption (MMMA) measurements were carried out with a Varian E-line ESR spectrometer operating in the X-band with an Oxford Instruments ESR 910 helium cryostat[10]. The substrates were fixed with silicone grease to the flat end of a Suprasil quartz holder. They were oriented with the microwave magnetic field B_{mw} perpendicular and the external magnetic field B_0 parallel to the substrate plane. B_0 was modulated with 100 kHz.

RESULTS: FILMS OF α-(BEDT-TTF)$_2$I$_3$

Scanning electron microscopy and X-ray diffraction spectra

First attempts in evaporating thin films onto silicon and quartz glass substrates were performed on substrates kept at room temperature and above in order to reproduce the results already obtained by Kawabata et al.[8,9].

At these temperatures the sticking coefficient of the incident molecules is small, requiring a high evaporation rate (working pressure 10^{-5} mbar) and a small source-target distance of only a few cm. Additionally the mobility of the adsorbed molecules is high, which results in the growth of single crystals with a size of a few μm. It can be

seen from Figure 1 that this mode of growth takes place on quartz glass as well as on silicon substrates. Whereas on the quartz glass small needles seem to grow, on the silicon substrate it looks like disordered leaves. Both substrates have been exposed to the molecular beam at the same time, so the observed differences in growth are due to the different substrate surfaces.

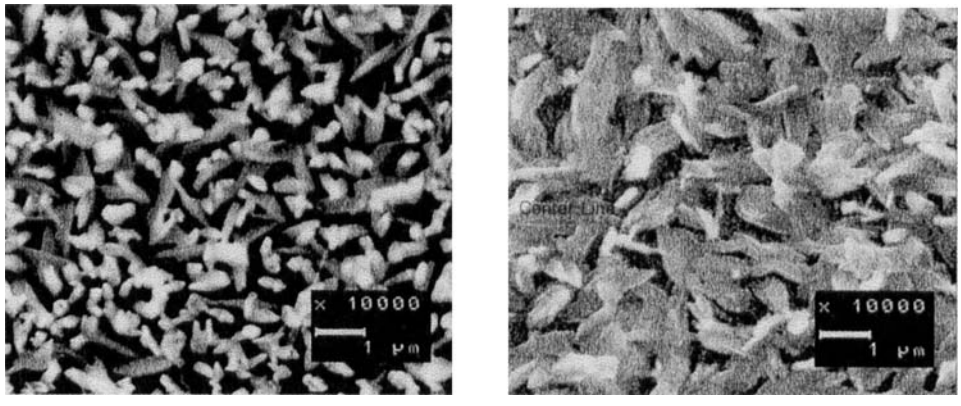

FIGURE 1 SEM micrographs of 1800 Å α-(BEDT-TTF)$_2$I$_3$ on quartz glass (left) and on silicon (right), evaporated at substrate temperatures of 300 K.

For a determination of the kind of crystals grown, X-ray diffraction spectra of both films were taken, which are shown in Figure 2. Though their look is rather different both films have the same diffraction spectra (aside from a weak underground which stems from scattering of the amorphous quartz substrate), and these spectra coincide in parts with the powder spectrum of α-(BEDT-TTF)$_2$I$_3$. With the knowledge of the unit cell of the α-phase[5] the expected reflexes can be calculated. From this the orientation of the unit cell with respect to the substrate plane can be determined, which is found to be (00l) i.e. the c^*-axis of the unit cell is perpendicular to the substrate plane. The resulting orientation of the unit cell with respect to the substrate plane is shown in Figure 3.
Concerning the powder spectrum of α-(BEDT-TTF)$_2$I$_3$ it should be mentioned that not all reflexes of low order (e.g. (h00) and (0k0)) are present. This is due to the plate-like morphology of the crystals, which prevents the occurrence of these orientations in the powder.
It has also been tried to produce α_t-phase by elevated substrate temperatures of about 70 °C, but due to the small evaporation rates only films consisting of neutral BEDT-TTF were obtained. At such substrate temperatures the sticking coefficient for the iodine molecules obviously is too small.

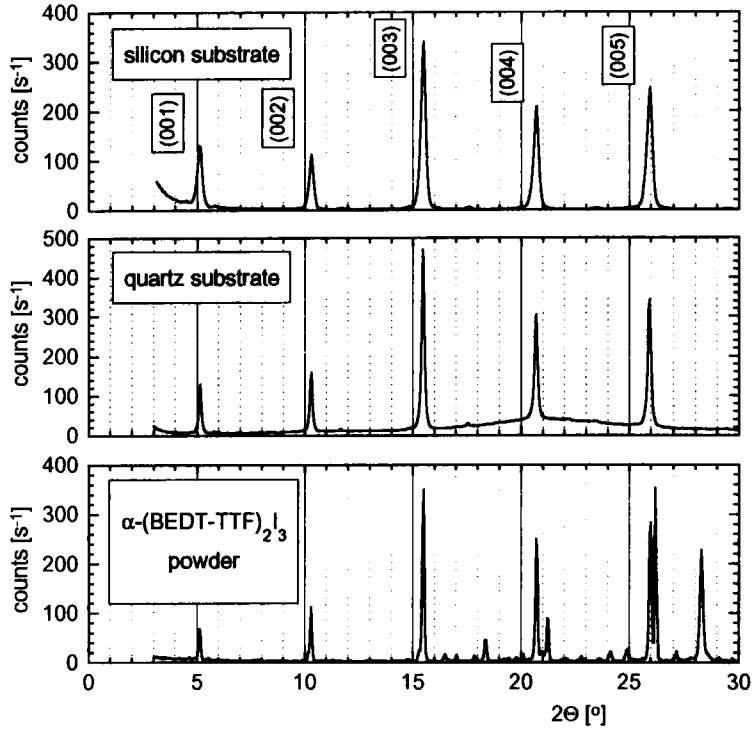

FIGURE 2 X-ray diffraction spectra of films, evaporated at room temperature: 2000 Å on silicon (above), 1800 Å on quartz glass (middle) and for comparison a powder spectrum of α-(BEDT-TTF)$_2$I$_3$.

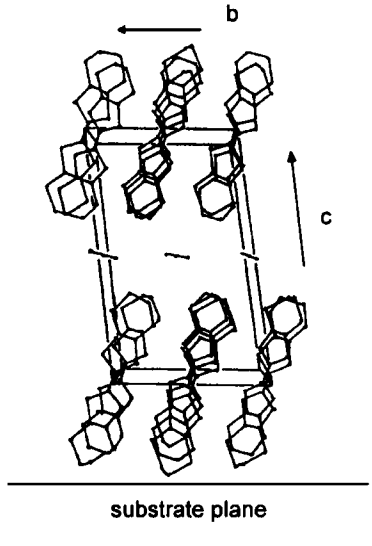

FIGURE 3 The unit cell of α-(BEDT-TTF)$_2$I$_3$ and its orientation with respect to the substrate plane as found in the evaporated films.

Substrate cooling

After the reproduction of the results already obtained by Kawabata et al. we tried to produce films which have a more smooth and a closed surface. This means to increase the sticking coefficient and simultaneously to reduce the mobility of the adsorbed molecules on the substrate which both can be achieved by the cooling of the substrate. The drawback of this method - i.e. cryopumping the residual gas with the substrate surface - was reduced by cooling a large area around the substrate at the same time with liquid nitrogen. The optimization of the evaporated films was achieved by the variation of a set of certain parameters, the result of which will be discussed in the next section.

Scanning electron microscopy

A first method to decide whether one is approaching the above mentioned aims is to investigate the produced films by SEM. Three of the best results obtained with different thickness at different substrate temperatures are shown in Figure 4 (the magnification is 5000). The defects of the films are either scratches or small particles which have been used to focus.

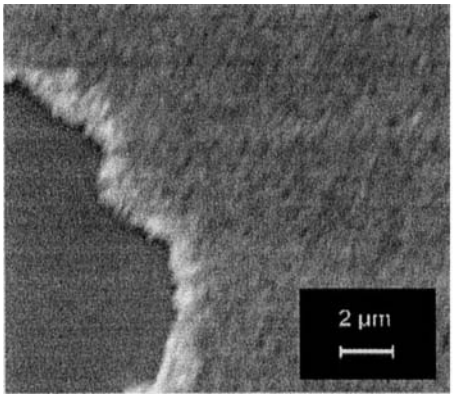

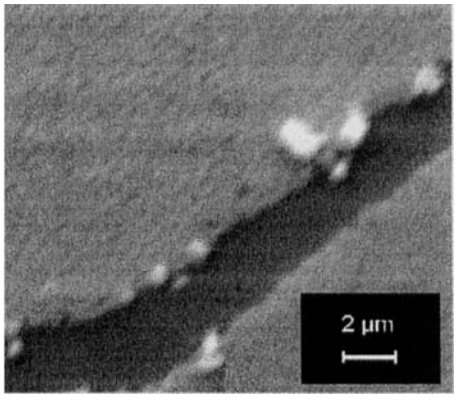

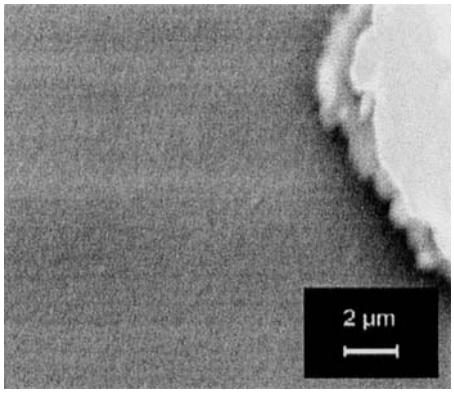

FIGURE 4 Scanning electron micrographs of several films of α-(BEDT-TTF)$_2$I$_3$ on silicon substrates at different temperatures T_{Sub} (see text).

Upper left: 2200 Å at T_{Sub}= 180 K
Upper right: 1500 Å at T_{Sub}= 150 K
Right: 2500 Å at T_{Sub}= 200 K

These films have been obtained by an optimization of the following parameters:

- The distance between the evaporation source and the substrate was around 10 cm.
- The optimum value of the substrate temperature was found to be lying between 150 K and 200 K, a further decrease showed no effect.
- The warming up rate of the substrate after evaporation was around 10 K/hour, which did not seem to be crucial. A hold and following annealing for a few hours at 250 K gave better results concerning crystallinity and orientation found in X-ray investigations (see below).
- For the evaporation rate the best values found were between 0.5 and 1.5 Å/s, which depend on the temperature at which the cell is opened and how long the evaporation is continued. It should be recalled that iodine evaporates at much lower temperatures than the BEDT-TTF molecules do.

X-ray diffraction

SEM investigations have shown that it is possible to produce films with a closed surface and a - compared to former results - strongly reduced roughness. Of course these films should consist of crystalline material with a defined stoichiometry - if additionally a preferred orientation with respect to the substrate plane is present, this should reveal itself in X-ray diffraction.

Figure 5 shows the X-ray diffraction spectra of two films on silicon and quartz glass - the one on silicon is shown in Figure 4 (upper left).

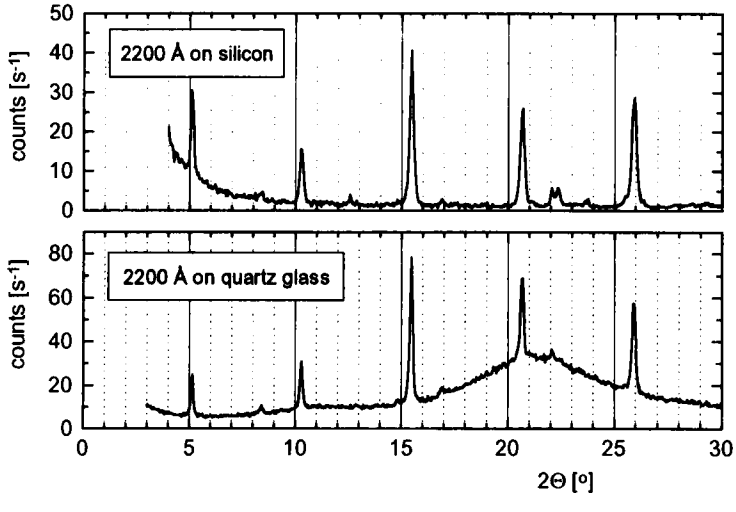

FIGURE 5 X-ray diffraction spectra of films evaporated onto silicon (above) and quartz glass (below) substrates kept at 180 K during the evaporation process.

Although the intensity of the diffracted beam is somewhat lower, the same reflexes as in Figure 2 (the films prepared with substrates at room temperature) are obtained. Therefore the films are still crystalline and oriented as already discussed before.

A closer look at the substrate surface by SEM (Figure 6) shows that even these smooth films show some roughness: they consist of a network of crystalline areas which sometimes are resolvable as single crystals and sometimes are grown into each other.

Concerning the degree of orientation of these crystalline areas, rocking curves have been recorded, one of which is shown in Figure 6 (left). The full width at half maximum (FWHM) of the rocking curve is below 1° which is a very good result for a non-epitactically grown film of organic material.

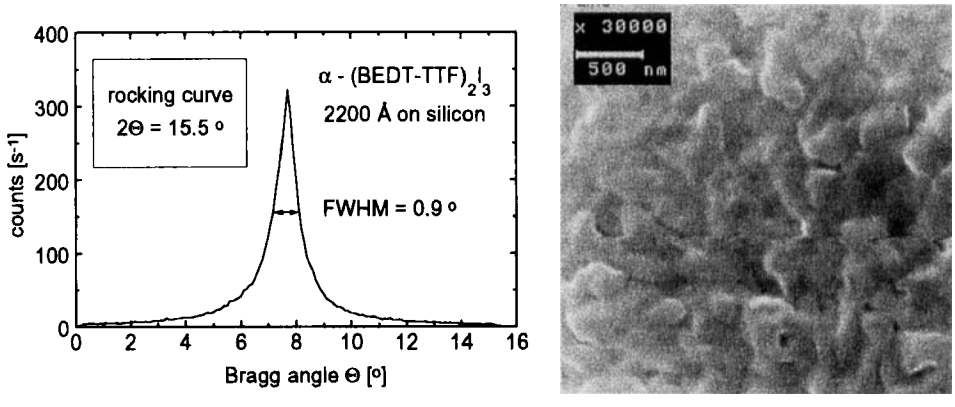

FIGURE 6 Rocking curve of the (003) reflex at 2Θ = 15.5° (left) and scanning electron micrograph of the same film with a magnification of 30000 (right).

FT-IR and Raman Investigations

From the results presented above it cannot be excluded that the film only partially consists of crystalline α-(BEDT-TTF)$_2$I$_3$ - disordered and non-stoichiometrical areas might be present, for example neutral BEDT-TTF. To investigate the bulk properties of the films IR-absorption and Raman spectra were recorded. With both methods the iodine salts of BEDT-TTF have been investigated extensively[11-14], so a comparison with the results from powder and crystals might give some insight.

Figure 7 shows the absorption spectra of an evaporated film of α-(BEDT-TTF)$_2$I$_3$ on silicon, α-(BEDT-TTF)$_2$I$_3$ powder and BEDT-TTF powder in a region where most of the vibrations of the BEDT-TTF molecule are observed.

The observed bands are numbered and the assignment is as follows: The bands 2 - 6 have been assigned[15,16] to various bending modes of the terminal CH_2 groups. Because the symmetry of the BEDT-TTF molecule is not exactly D_{2h} and the deviation from

ideal flatness depends on the average charge on the molecule, these bands are not very useful for our purposes. In comparison the bands No. 1 and No. 7 belong to vibrations of the BEDT-TTF framework and both have symmetry B_{1u}.

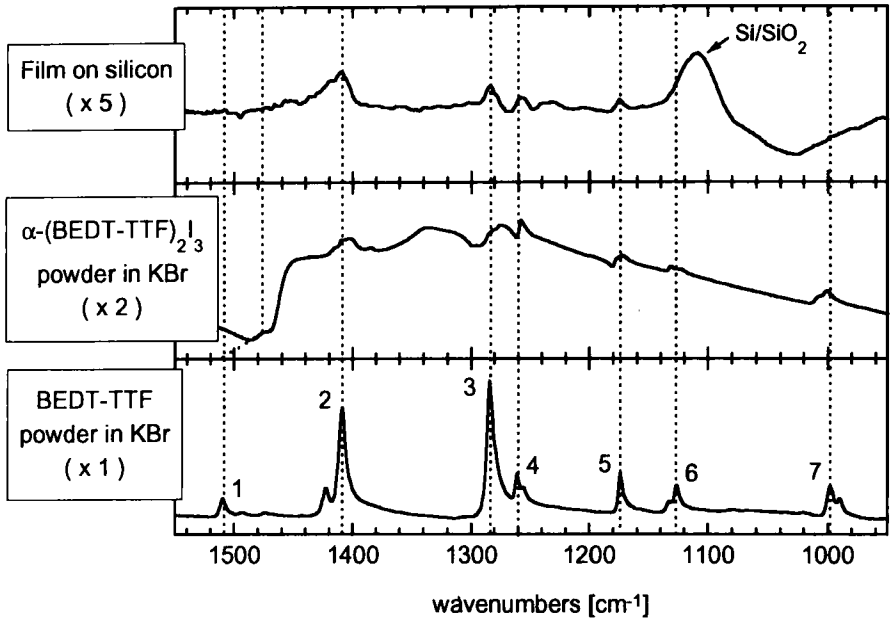

FIGURE 7 Infrared absorption spectra of a film on silicon (above), α-(BEDT-TTF)$_2$I$_3$ powder in KBr (middle) and neutral BEDT-TTF powder in KBr (below) (see text).

Vibration No.1 is an antisymmetric stretching of the ring C=C bonds and No. 7 belongs to the antisymmetric stretching vibration of the outer C-C groups (see Figure 8). The frequency of the former is strongly dependent on the average charge upon the molecule[13]. It shifts from 1509 cm^{-1} in the neutral BEDT-TTF molecule to 1477 cm^{-1} in the 2:1 radical salts (where it is very weak) and to 1445 cm^{-1} in the BEDT-TTF$^+$ cation. The absence of this band in the spectrum of the film (Figure 7) shows that the fraction of neutral BEDT-TTF contained in the films is negligible. The same applies for the absence of the (charge-independent) vibration No. 7 around 1010 cm^{-1}.

If there were disordered regions in the film, vibration No. 7 should be as well present in the spectrum. If instead all molecules are oriented in the way found from X-ray diffraction, the resulting dipole moment is always nearly perpendicular to the electric field of the radiation (see Figure 8). The absence of this band in the spectrum of the film indicates that no regions with disordered α-(BEDT-TTF)$_2$I$_3$ are present in the films.

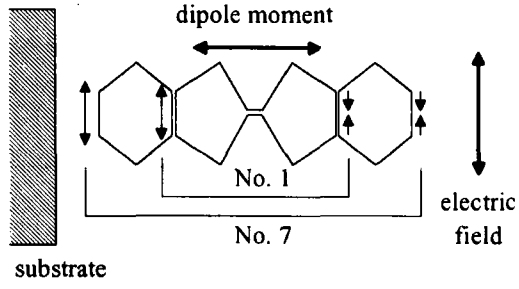

FIGURE 8 Electric field of IR-radiation and dipole moment of vibrations No. 1 and No. 7 in an oriented BEDT-TTF molecule.

Another method of determining whether the stoichiometry of the deposited material is correct is Raman scattering. The Raman spectra of the main phases of $(BEDT\text{-}TTF)_2I_3$ are known[14] and serve as fingerprints for their identification as well as IR spectra.

Figure 9 shows the low energetic part of Raman spectra of a film on silicon, an α-$(BEDT\text{-}TTF)_2I_3$ crystal and of BEDT-TTF powder. Aside from a broadening of the lines the spectra of the α-$(BEDT\text{-}TTF)_2I_3$ crystal and of the film are the same. Additionally no bands from the neutral donor are observed in the film, which again shows that no significant amount of neutral BEDT-TTF is present in the films.

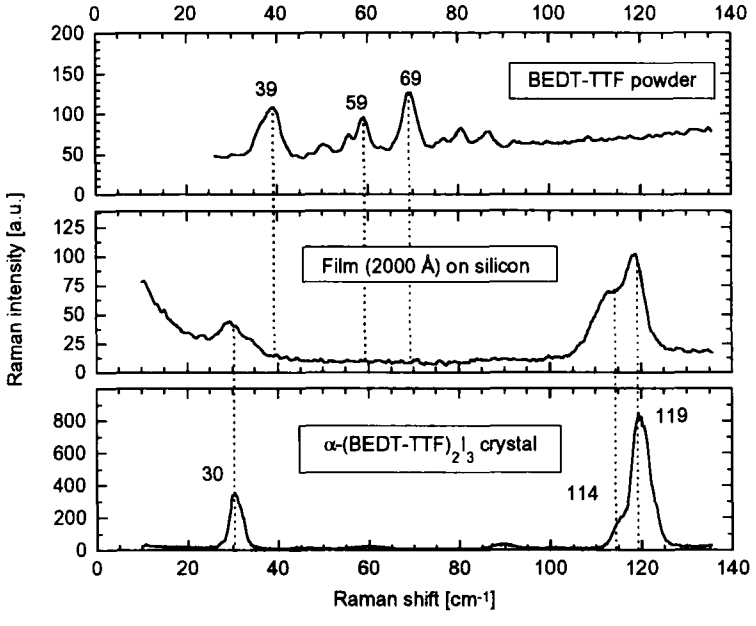

FIGURE 9 Raman spectra of a film on silicon (middle), an α-$(BEDT\text{-}TTF)_2I_3$ crystal (below) and BEDT-TTF powder (above).

Dc-Conductivity

One of the aims in preparing thin films of organic conductors and superconductors is to obtain the same transport properties as found in single crystals. Therefore measurements of the dc-conductivity of films on non-conducting materials (quartz glass) were made. The result is shown in the upper part of Figure 10. A thermally activated behavior is found over the whole temperature region from 300 K to 90 K. Between 300 K and 160 K the activation energy is 420 meV, below 160 K it is found to be 580 meV. In a single crystal of α-(BEDT-TTF)$_2$I$_3$ the conductivity is metallic until 135 K with a maximum at 160 K (see lower part of Figure 10). Then a sharp metal-insulator phase transition takes place and below 100 K the conductivity of the crystal and the film become equal.

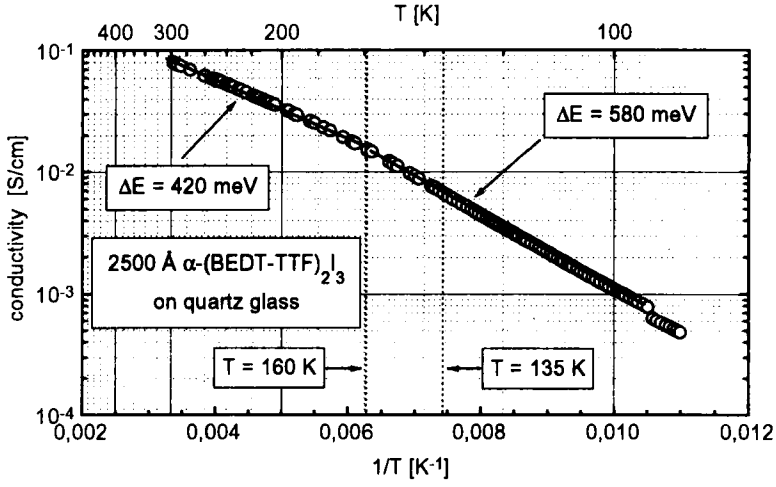

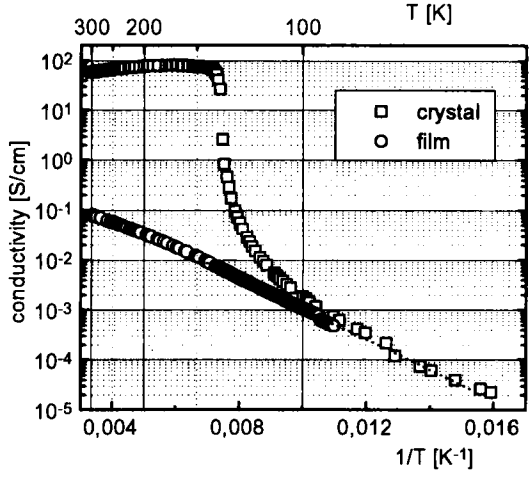

FIGURE 10 Arrhenius plot of the conductivity of a film of α-(BEDT-TTF)$_2$I$_3$ (above) and comparison between conductivity of the film and of a α-(BEDT-TTF)$_2$I$_3$ single crystal (right) (the dotted line is an extrapolation of the conductivity of the film below 90 K).

This thermally activated behavior obviously stems from grain boundaries between the microcrystals constituting the film, as seen in Figure 6. It seems that growth on the cooled substrates starts at many points and leads to the formation of many grains.
Another reason might be the fact that the conduction layers in the film are parallel to the substrate, so that the electrons have to pass a lot of iodine layers before reaching the full cross-sectional area of conducting planes.

THE TRANSFORMATION INTO α_t-(BEDT-TTF)$_2$I$_3$

Concerning electric conductivity α-(BEDT-TTF)$_2$I$_3$ suffers from the disadvantage that a metal-insulator transition takes place at 135 K. The thermally converted α_t-(BEDT-TTF)$_2$I$_3$ instead remains metallic down to low temperatures until 8 K, where a superconducting transition takes place[6,7].
Because this tempering process obviously destroys the surface of the crystals by a loss of iodine (leaving orange spots of neutral BEDT-TTF), some caution is necessary in converting the thin films. Whereas the conversion of crystals is carried out by tempering at 75 °C for 2 or 3 days, it was found that the best results - i.e. complete conversion of the α-(BEDT-TTF)$_2$I$_3$ films with minimum destruction of the film - are obtained by tempering the films only for 1 to 3 hours but at 85 °C to 90 °C .

X-ray diffraction

The result of the thermal conversion of a film on silicon is shown in Figure 11, where a clearly visible shift of the reflexes to larger values of 2 Θ (i.e. smaller distance of reflecting planes) has taken place. Thus the converted films are crystalline and oriented with respect to the substrate surface.
An examination of the crystal structure of α_t-(BEDT-TTF)$_2$I$_3$ and the obtained reflexes in X-ray diffraction yield an orientation of the unit cell with respect to the substrate plane as shown in Figure 12. Here - as before with α-(BEDT-TTF)$_2$I$_3$ - the c*-axis of the unit cell is perpendicular to the substrate surface, which means that no reorientation of the unit cell has taken place, only the unit cell itself has changed.
The mechanical stability of the films has been checked by scanning electron microscopy. There were no changes visible in the first 3 hours of tempering - only if the time of exposure reached 6 or more hours, holes were growing in the film. A closer examination by atomic force microscopy revealed[17], that the single crystals are getting larger and therefore the roughness of the film increases if temper time exceeds 3 hours.

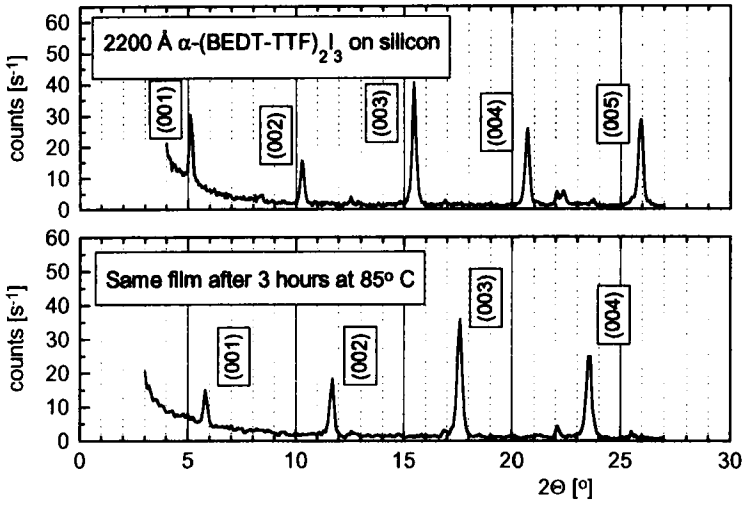

FIGURE 11 X-ray diffraction spectra of a film evaporated onto silicon (above) and the same film after a three-hour thermal conversion at 85 °C (below).

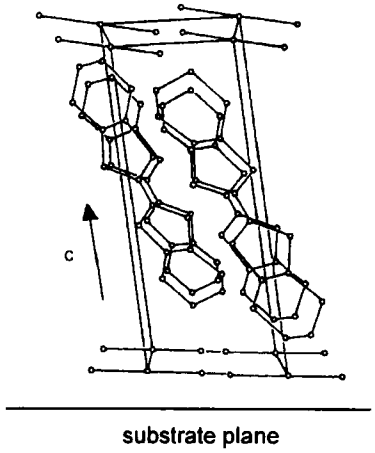

FIGURE 12 The unit cell of α_t-(BEDT-TTF)$_2$I$_3$ and its orientation with respect to the substrate plane as obtained in the thermally converted films.

Dc-Conductivity

Since the thermally converted α_t-phase is metallic until 8 K and superconducting below, measurements of the dc-conductivity on converted films were carried out. A typical result is shown in Figure 13 (upper part). The dc-conductivity is still thermally activated with an activation energy (555 meV) even higher than the one obtained for α-(BEDT-TTF)$_2$I$_3$ films in the metallic region (420 meV). It is not likely that the decreased room temperature conductivity (see Figure 10) stems from the conducting grains of α_t-(BEDT-TTF)$_2$I$_3$ itself. As already seen from AFM investigations, the

temper process seems to increase the size of the grains and also to reduce the conductivity between them. A closer examination of the temper process as shown in Figure 13 confirms this assumption. As the temperature of the film rises the resistance falls according to the thermal activation. Above 70 °C this drop of resistance stops immediately and the resistance begins to rise until it saturates nearly two orders of magnitude above its initial value.

If after that the temperature is again decreased to room temperature (not shown in Figure 13), the film resistance again increases half an order of magnitude due to the thermal activation. After that the whole procedure can be repeated with the same results i.e. a significant loss of conductivity with each cycle of tempering. Because the elastic constants of the film and the substrate are not known yet, a part of this increase in resistivity might be due to cracks in the film most likely during the heating cycle (remember the distance between contacts is as large as 0.2 mm).

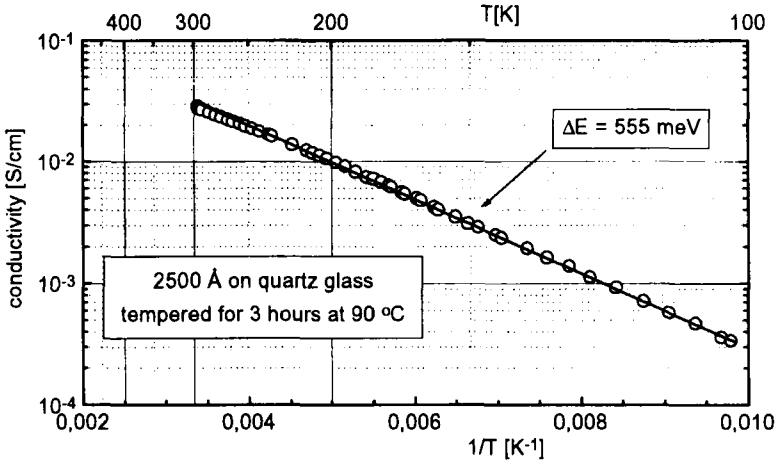

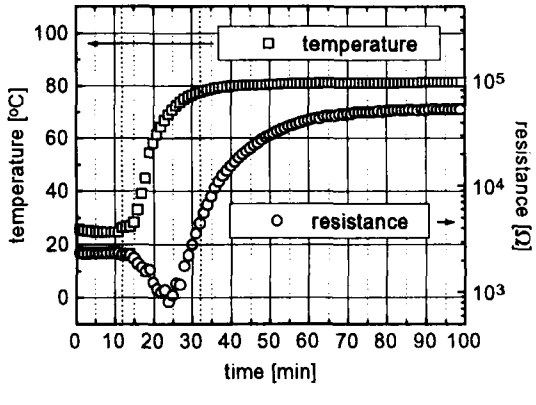

FIGURE 13 Arrhenius plot of the conductivity of a film of α_t-(BEDT-TTF)$_2$I$_3$ (above) and the evolution of film resistance as a function of temperature and time (right) (see text).

Magnetically modulated microwave absorption

Because a direct detection of the superconductivity by a measurement of the dc-conductivity is not possible in films consisting of many grains, the method of microwave absorption in a low magnetic field was applied. This method was successfully applied with granular high temperature superconductors[18,19] and superconductors of the BEDT-TTF family[10,20,21]. An explanation of the mechanism of this absorption process linked with the superconducting transition has been given by Dulcic et al.[22,23] and is based on the analysis of a network of superconducting grains coupled by Josephson junctions.

In the upper left part of Figure 14 a typical absorption signal of a superconducting film of α_t-(BEDT-TTF)$_2$I$_3$ at 1.7 K is shown.

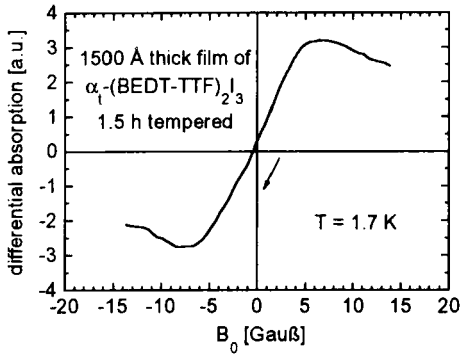

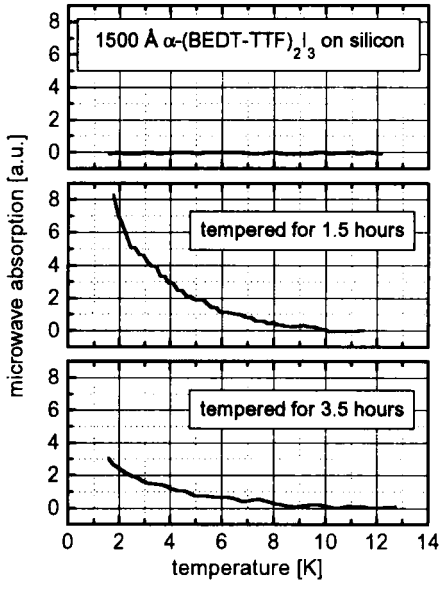

FIGURE 14 Low field modulated microwave absorption: Field sweep at 1.7 K (above) and temperature dependence for three different films at B_0 = 14 G (right side).

To assure that this signal is really due to superconductivity in the film, we measured a batch of films which have been treated differently. The main result is shown in the right part of Figure 14. There is no signal found in the not tempered film of α-(BEDT-TTF)$_2$I$_3$, whereas maximum signal strength is obtained in films which have been tempered between 1 and 2 hours. Further exposition to temperatures around 90 °C results in a decrease of the signal strength until it vanishes after 6 and more hours.

It is evident that films of α_t-(BEDT-TTF)$_2$I$_3$, tempered between 1 and 2 hours at 90 °C show an onset of superconductivity at around 9 K, e.g. at the same temperature as crystals of α_t-(BEDT-TTF)$_2$I$_3$. At the present state the films of α_t-(BEDT-TTF)$_2$I$_3$ are

smooth and cover the substrate completely but still consist of single grains. There are, however, indications (see next chapter) that - by choosing the right substrate and improving the evaporation conditions - epitactical growth is possible.

FILMS OF $(BEDO\text{-}TTF)_{2.4}I_3$

From the iodine salt of BEDO-TTF only one phase is known to date. $(BEDO\text{-}TTF)_{2.4}I_3$[2] has a composite structure with two interpenetrating lattices formed by BEDO-TTF and the triiodide counteranions. Both sublattices have a different periodicity in the b-axis direction - the unit cell is shown as a part of Figure 18 in the b-axis projection, which is coincident for both lattices.

First tests of the evaporation dynamics of $(BEDO\text{-}TTF)_{2.4}I_3$ showed that the iodine component starts evaporating from the crystal around 70 °C and the evaporation of BEDO-TTF begins around 130 °C. This is much earlier than with BEDT-TTF and should give a more correct stoichiometry in the molecular beam.

Scanning electron microscopy

SEM micrographs of different films evaporated onto different substrates are shown in Figure 15.

The first films on silicon substrates gave results as shown in the upper left picture of Figure 15, i.e. irregular arrangements of small needles with a size of 1 μm or less - films evaporated onto quartz glass have the same appearance.

After that film growth on different substrates like NaCl single crystals was investigated. The result of the deposition of 550 Å onto an NaCl single crystal at 250 °C is shown in the upper right part of Figure 15. Obviously the film is not smooth - a network of rectangular arrangement of small crystals is clearly visible. This growth mode can be explained by the cubic lattice of the NaCl substrate. The bright spots are indicating that some needles are growing perpendicular to the substrate.

Much better results on NaCl single crystals, however, are obtained with a special two-stage evaporation process, i.e. a few 100 Å were deposited at substrate temperatures around 200 K. After heating the substrate to room temperature, another few 100 Å were evaporated onto the existing film. Such a film is shown in the lower part of Figure 15. It has an absolutely smooth surface (aside from an edge that was used to focus).

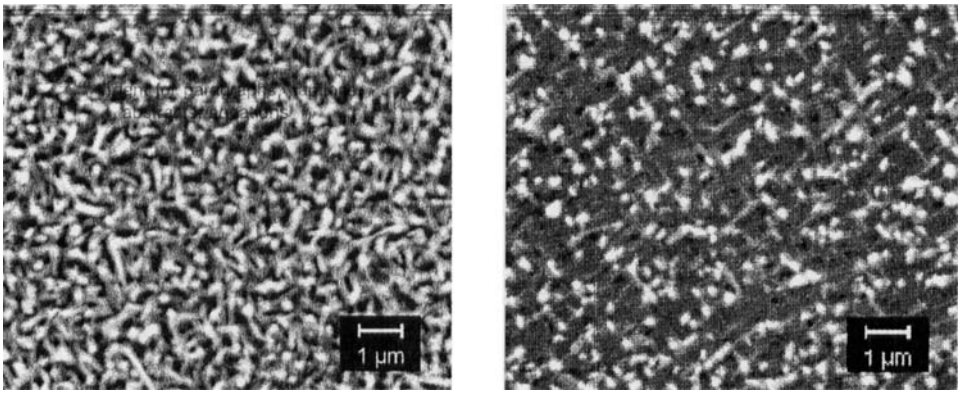

FIGURE 15 A film of 400 Å $(BEDO\text{-}TTF)_{2.4}I_3$ on silicon at 220 °C (upper left), 550 Å on an NaCl single crystal at 250 °C (upper right) and 600 Å on an NaCl single crystal, evaporated in a two-stage process (right) (see text). Magnification: 10000

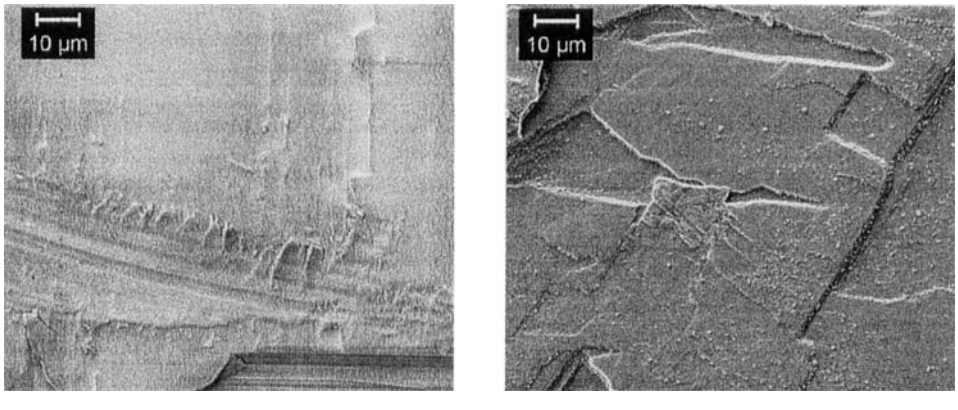

FIGURE 16 Enlarged view of a film on NaCl, which was evaporated in a two stage process (left) (see text). For comparison, the surface of a $(BEDO\text{-}TTF)_{2.4}I_3$ single crystal is shown in the right picture. Magnification: 1000.

In Figure 16 (left picture) a larger area of the same film is shown, in which some macroscopic damages can be recognized. Additionally the film is mechanically stable, i.e. it can be removed from the substrate without damaging it. For comparison the surface of a $(BEDO\text{-}TTF)_{2.4}I_3$ single crystal is shown as well in Figure 16.

X-ray diffraction

Further results on the quality of such films are obtained by X-ray diffraction. Figure 17 shows three spectra of films on different substrates. The first (lower spectrum) shows the spectrum of a 800 Å thick film on a quartz glass substrate. Two distinct Bragg peaks can be seen - therefore at least two different orientations of the crystalline material with respect to the substrate plane are present in the film. The second (middle of Figure 17) shows the spectrum of a 400 Å thick film on a silicon wafer, on which only one orientation of the crystalline material is found.

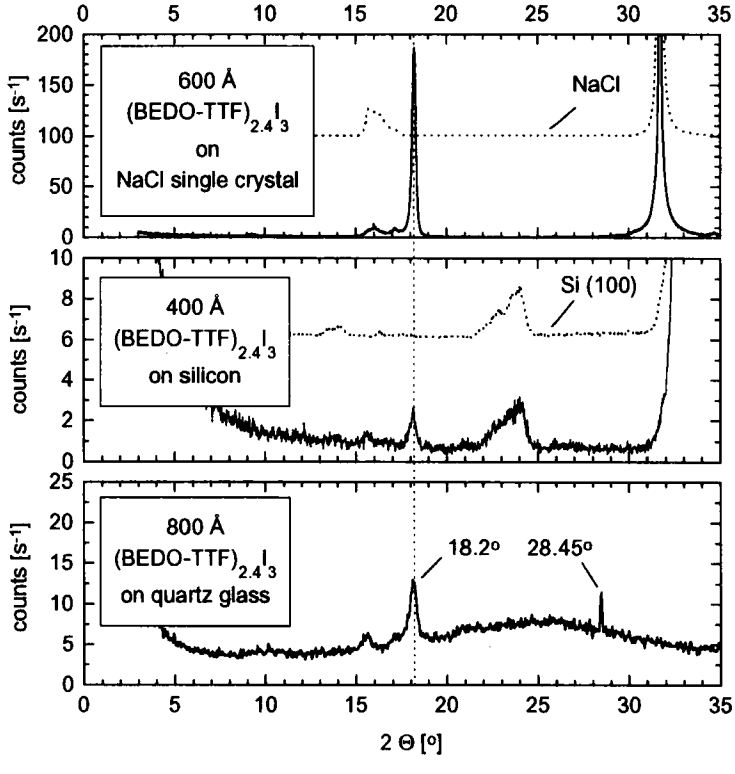

FIGURE 17 X-ray diffraction spectra of a 800 Å thick film of $(BEDO\text{-}TTF)_{2.4}I_3$ on quartz glass (below), a 400 Å thick film on Si (100) and a 600 Å thick film on NaCl (the dotted lines are from uncovered substrates).

The sublattices of donor and anion are incommensurate in the b-direction[2], but the (h0l) planes coincide. Here the observed Bragg angle of 18.2° yields a $(10\bar{1})$ orientation of the reflecting planes.

Both reflexes at 18.2° in the above mentioned films are weak in contrast to the one obtained from the film on the NaCl substrate (upper spectrum), which was shown in Fig. 15, right picture. The reflex from the film is nearly as strong as the (200) reflex from the substrate at 31.8°, which confirms the result obtained from SEM of large, nearly perfect crystalline areas.

The resulting orientation of the unit cell of $(BEDO\text{-}TTF)_{2.4}I_3$ with respect to the substrate plane is shown in Fig. 18. One should notice, that the BEDO-TTF molecule is now lying on the substrate surface, in contrast to the standing BEDT-TTF molecules in films of $(BEDT\text{-}TTF)_2I_3$. In this orientation, the repetition length of the iodine anions is about 17.4 A, which is 3.1 times the distance of the sodium atoms on the substrate surface. Maybe this match is the reason for the observed orientation.

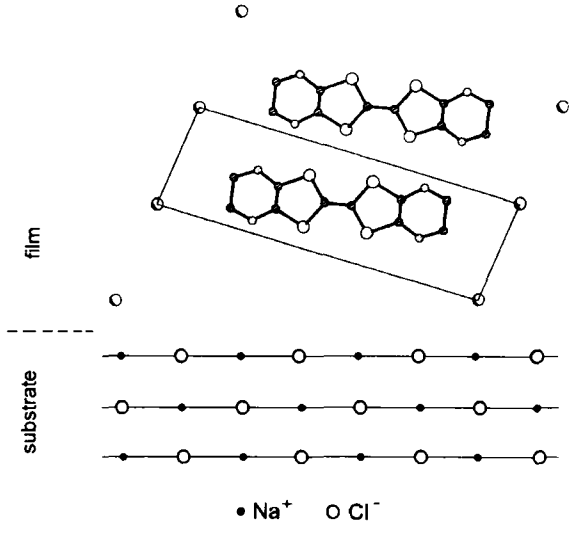

FIGURE 18 The unit cell of $(BEDO\text{-}TTF)_{2.4}I_3$ (view down the b-axis)[2], its orientation in the film on NaCl and the lattice of the NaCl substrate. The I_3^- molecules are at the corners of the unit cell.

Dc-Conductivity

As seen from the films of α-$(BEDT\text{-}TTF)_2I_3$ their dc-conductivity was thermally activated, which is due to the presence of grain boundaries between the microcrystals forming the film. In Figure 19 the dc-conductivity of two $(BEDO\text{-}TTF)_{2.4}I_3$ films is shown. The first (lower graph) is a film on quartz glass with a very rough surface as shown in Figure 15 (upper left). Although the room temperature conductivity is in the order of that of $(BEDT\text{-}TTF)_2I_3$ film (2-3 orders of magnitude below that of crystals), the value of the activation energy is much smaller (50 meV).

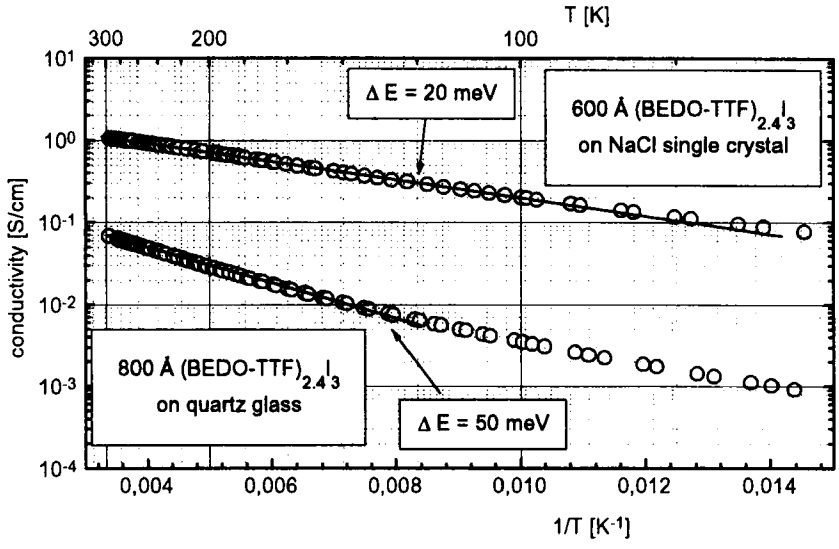

Figure 19 Dc-conductivity versus 1/T of a film of $(BEDO\text{-}TTF)_{2.4}I_3$ (800 Å) on quartz glass (below) and of 600 Å on an NaCl single crystal (above).

In the second film, which is the very smooth film on NaCl (upper graph in Figure 19) the activation energy is only 20 meV and the room temperature conductivity is 1 S/cm, i.e. only one order of magnitude below that of single crystals of $(BEDO\text{-}TTF)_{2.4}I_3$. Taking into account that the conducting planes are not parallel to the substrate plane and that there are mechanical defects in the film surface (see micrograph in Figure 6), this is a very good value.

Raman spectroscopy

Because the Raman spectra of the symmetric stretching vibration of the I_3^- - anion have always served as reliable fingerprints for the determination of crystallographic phases in radical cation salts of BEDT-TTF [12,24], we used this method to make sure that the films definitely consist of $(BEDO\text{-}TTF)_{2.4}I_3$. The Raman spectra of $(BEDO\text{-}TTF)_{2.4}I_3$ powder and the films on quartz and NaCl are shown in Figure 20. The band at 112 cm^{-1} is the same as in the powder. The origin of the band at 137 cm^{-1} is not clear yet. We have made sure that this band does not originate from neutral BEDO-TTF, or from any of the substrates. The frequency of this band indicates that it is due to a triiodide anion which is not linear or to the presence of I_5^--anions.

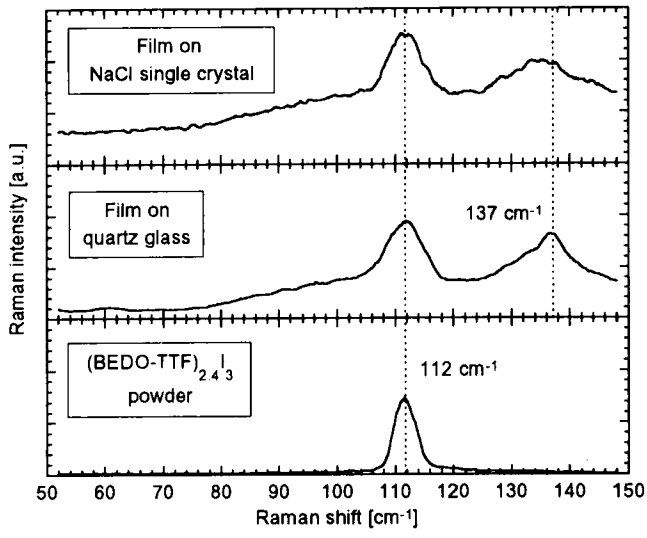

FIGURE 20 Raman spectra of the symmetric I_3^- stretching vibration of $(BEDO\text{-}TTF)_{2.4}I_3$ powder (below), a film on quartz glass (middle) and a film on NaCl (above).

Summary and conclusions

We have investigated the possibilities to produce thin films of triiodide salts of BEDT-TTF and BEDO-TTF. With the evaporation of $(BEDT\text{-}TTF)_2I_3$ crystals it is possible to obtain crystallization of α-$(BEDT\text{-}TTF)_2I_3$ on substrates. Even if these films consist of very small single crystals, XRD reveals that they have a very high degree of orientation with respect to the substrate plane. Under suitable conditions like cooled substrates these films have a closed surface and are relatively smooth. Scanning electron microscopy reveals that these films still consist of grains. Therefore the dc-conductivity is thermally activated. Infrared- and Raman spectroscopy show that the films have a homogeneous composition with no significant defects in stoichiometry. Under special tempering conditions it is possible to convert the films into α_t-$(BEDT\text{-}TTF)_2I_3$. MMMA investigations show that the films of α_t-$(BEDT\text{-}TTF)_2I_3$ become superconducting with an onset at 9 K.

Taking into account the structure of the substrate surface, it is possible to obtain films with a high quality as shown with $(BEDO\text{-}TTF)_{2.4}I_3$ on NaCl single crystals.

With the step to UHV conditions ($p < 10^{-10}$ mbar) and the right choice of substrates we are confident that epitactical growth is possible.

REFERENCES

1. G. Saito, T. Enoki, K. Toriumi, H. Inokuchi, Solid State Comm., 42, 557 (1982).
2. F. Wudl, H. Yamochi, T. Suzuki, H. Isotalo, C. Fite, H. Kasmai, K. Liou, G. Srdanov, P. Coppens, K. Maly, A. Frost-Jensen, J. Am. Chem. Soc., 112, 2461 (1990).
3. see J. M. Williams, J. R. Ferraro, R. J. Thorn, K. D. Carlson, U. Geiser, H. H. Wang, A. M. Kini, M.-H. Whangbo, Organic Superconductors (Including Fullerenes) - Synthesis, Structure, Properties, and Theory (Prentice Hall, New Jersey, 1992).
4. K. Bender, K. Dietz, H. Endres, H. W. Helberg, I. Hennig, H. J. Keller, H. W. Schäfer, D. Schweitzer, Mol. Cryst. Liq. Cryst., 107, 45 (1984).
5. K. Bender, I. Hennig, D. Schweitzer, K. Dietz, H. Endres, H. J. Keller, Mol. Cryst. Liq. Cryst., 108, 359 (1984).
6. G. O. Baram, L. I. Buravov, L. C. Degtariev, M. E. Kozlov, V. N. Laukhin, E. E. Laukhina, V. G. Orischenko, K. I. Pokhodnia, M. K. Scheinkman, R. P. Shibaeva, E. B. Yagubskii, JETP Lett., 44, 293 (1986).
7. D. Schweitzer, P. Bele, H. Brunner, E. Gogu, U. Haeberlen, I. Hennig, T. Klutz, R. Swietlik, H. J. Keller, Z. Phys. B Condensed Matter, 67, 489 (1987).
8. K. Kawabata, K. Tanaka, M. Mizutani, Solid State Comm., 74, 83 (1990).
9. K. Kawabata, K. Tanaka, M. Mizutani, Synth. Metals, 41-43, 2097 (1991).
10. P. Bele, H. Brunner, D. Schweitzer, H. J. Keller, Solid State Comm., 92, 189 (1994).
11. R. Zamboni, D. Schweitzer, H. J. Keller, C: Taliani, Z. Naturforsch., 44, 295 (1989).
12. J. Moldenhauer, K. I. Pokhodnia, D. Schweitzer, I. Heinen, H. J. Keller, Synth. Metals, 55-57, 2548 (1993).
13. J. Moldenhauer, Ch. Horn, K. I. Pokhodnia, D. Schweitzer, I. Heinen, H. J. Keller, Synth. Metals, 60, 31 (1993).
14. R. Swietlik, D. Schweitzer, H. J. Keller, Phys. Rev. B, 36, 6881 (1987).
15. M. E. Kozlov, K. I. Pokhodnia, A. A. Yurchenko, Spectrochim. Acta A, 43, 323 (1987).
16. M. E. Kozlov, K. I. Pokhodnia, A. A. Yurchenko, Spectrochim. Acta A, 45, 437 (1989).
17. J. Moldenhauer, H. Wachtel, D. Schweitzer, B. Gompf, W. Eisenmenger, P. Bele, H. Brunner, H. J. Keller, Synth. Metals, 70, 791 (1995).
18. S. H. Glarum, J. H. Marshall, L. F. Schneemeyer, Phys. Rev. B, 37, 7491 (1988).
19. A. Dulcic, B. Leontic, M. Peric, B. Rakvin, Europhys. Lett., 4, 1403 (1987).
20. M. Thakur, R. C. Haddon, S. H. Glarum, J. Cryst. Growth, 106, 724 (1990).
21. R. C. Haddon, S. H. Glarum, S. V. Chichester, A. P. Ramirez, N. M. Zimmerman, Phys. Rev. B, 43, 2642 (1991).
22. A. Dulcic, B. Rakvin, M. Pozek, Europhys. Lett., 10, 593 (1989).
23. M. Pozek, A. Dulcic, B. Rakvin, Physica C, 169, 95 (1990).
24. R. Zamboni, D. Schweitzer, H. J. Keller, Solid State Comm., 73, 41 (1990).

We gratefully acknowledge financial support of this work by the Deutsche Forschungsgemeinschaft (SFB 329).